Modulation of single-channel properties of TRPV1 by phosphorylation

Milena Studer and Peter A. McNaughton

Department of Pharmacology, University of Cambridge, Cambridge CB2 1PD, UK

Activation of TRPV1, the heat and capsaicin receptor, is known to be promoted by phosphorylation, but the molecular details are unclear. In the present study we recorded from single TRPV1 ion channels using the cell-attached patch clamp technique. The influence of capsaicin concentration on the time constants of open and closed states demonstrates the existence of at least four closed and three open states, and shows that channel opening can occur from partially liganded states. Activation of protein kinase C (PKC) promotes channel opening in some channels but not others, consistent with some channels being inaccessible to the kinase. The changes in open and closed state time constants following activation of PKC are equivalent to an increased affinity of capsaicin binding, but other arguments suggest that channel opening must be potentiated by downstream changes in channel activation rather than by a direct action of phosphorylation on the capsaicin binding site. Mutation of functionally important PKC phosphorylation sites on TRPV1, or application of staurosporine, a broad-spectrum kinase inhibitor, completely inhibited the effect of PKC in enhancing channel open time. Staurosporine also inhibited channel activity in the absence of overt PKC activation, showing that TRPV1 is partially phosphorylated at rest. This study elucidates the mechanism by which phosphorylation by PKC potentiates the activation of single TRPV1 ion channels.

Introduction

The ion channel TRPV1 is expressed in primary sensory neurons and is activated by a broad range of stimuli, including painful levels of heat, capsaicin (the active ingredient of chilli peppers), protons and endogenous factors such as anandamide (Caterina *et al.* 1997; Tominaga *et al.* 1998; Zygmunt *et al.* 1999; Premkumar & Ahern, 2000; Vellani *et al.* 2001). TRPV1 is critical for the increase in sensitivity to heat which is observed following inflammation, because this *inflammatory hyperalgesia* is absent in mice from which TRPV1 has been genetically deleted (Caterina *et al.* 2000; Davis *et al.* 2000).

Inflammatory hyperalgesia is initiated by inflammatory mediators, such as bradykinin, nerve growth factor (NGF) and PGE$_2$, released from damaged or stressed tissues. Interaction of these mediators with their cell surface receptors causes activation of downstream kinases such as PKCε, PKA and Src, and these kinases in turn phosphorylate specific serine, threonine or tyrosine residues in the intracellular domains of TRPV1 (reviewed in Huang *et al.* 2006). Two separate effects

of phosphorylation on TRPV1 have been distinguished in whole-cell recordings: a lowering of the thermal threshold for activation of TRPV1, and in parallel an enhancement in its sensitivity to other activating factors such as capsaicin, protons and anandamide (Vellani *et al.* 2001); and an increased trafficking of TRPV1 channels to the surface membrane (Morenilla-Palao *et al.* 2004; Zhang *et al.* 2005). Whole-cell recordings can inform us about the broad features of TRPV1 activation, such as the thermal activation threshold, but detailed mechanistic information about the numbers of steps involved in channel activation, and which of these steps may be modulated by phosphorylation to enhance channel activation, can only be obtained from analysis of the gating of single ion channels. Electrophysiological recordings at the single-channel level have revealed details of the mechanisms of activation of TRPV1 by capsaicin, heat and low pH (Premkumar *et al.* 2002; Hui *et al.* 2003; Liu *et al.* 2003; Ryu *et al.* 2003), but the mechanism by which phosphorylation enhances TRPV1 channel activation has not to date been investigated at the single-channel level.

The aim of this work was to use a kinetic analysis of single-channel activity to gain a better understanding of the mechanisms involved in TRPV1 gating, and of its modulation by phosphorylation. The main questions we sought to answer are: Does phosphorylation enhance single-channel activity? Does phosphorylation affect particular stages in channel opening, and can clues to the molecular mechanism of action be gained from this? Are all channels affected equally by phosphorylation?

Methods

Cell culture and transient transfection

HEK 293 cells were obtained from the European Collection of Cell Cultures ECACC, and were maintained in Dulbecco's modified Eagle medium (Invitrogen) supplemented with 10% fetal bovine serum at 37°C, 5% CO_2. For patch clamp experiments, cells were plated onto 6 mm diameter glass cover-slips coated with poly-D-lysine at a density of 50,000 cells ml^{-1} and transfected 24 h after plating using calcium phosphate (CalPhos, Clontech) according to the manufacturer's protocol, but with a shorter incubation period (2 h) and a low concentration of TRPV1 plasmid DNA (0.4 μg per 4-well plate) in order to minimise channel expression and thus to maximise the frequency of encountering single channels. Constructs used for transfection were hTRPV1 and the hTRPV1 S502A/S801A double mutant cloned in a pcDNA 3.1/ V5-His TOPO vector (Invitrogen). The TRPV1 S502A/S800A double mutant was constructed using the mega-primer PCR method, and the mutations were confirmed by sequencing (Zhang *et al.* 2005). Both constructs were co-transfected with green fluorescent protein (GFP; Clontech), in a ratio of 1 TRPV1 to 10 GFP, as a marker for transfected cells.

Acquisition of single-channel recordings

Single TRPV1 channels were recorded in the cell-attached configuration so that the influence of cell signalling pathways could be studied. The cell membrane (other than under the patch pipette) was maintained at 0 mV with a high-K$^+$ extracellular solution. Capsaicin was applied via the patch pipette (except in Fig. 2*C*) to prevent activation of channels elsewhere in the cell, which may have increased the noise of recording. As capsaicin activates TRPV1 at an intracellular site (Jung *et al.* 1999; Jordt & Julius, 2002) it is likely that this configuration would have led to a lower capsaicin concentration at its binding site.

Electrophysiological experiments were performed 18–48 h after transfection, and only one cell per cover-slip was used. Recordings were made at room temperature (22°C) using an Axopatch 200B amplifier and pCLAMP

9 software (Axon Instruments). Pipettes were made from thick-walled borosilicate glass (Clark Instruments 150F-10, Harvard Apparatus) using a horizontal two-stage puller (Flaming Brown micropipette puller model P-80/PC), and pipettes were coated with Sylgard 184 (Dow Corning) to minimise pipette capacitance (Gibb, 1995). To facilitate gigaseal formation pipette tips were fire-polished (Narishige microforge, model MF-830) before use. The pipette resistance was 10–15 MΩ when filled with pipette solution consisting of (in mM): sodium gluconate 140, NaCl 10, MgCl$_2$ 1, Hepes 5, EGTA 1.5, pH adjusted to 7.3 with NaOH.

Cover-slips with transfected cells were placed in a fast-exchange perfusion chamber (RC-24N, Warner Instruments) with a volume of 50 μl. Keeping the solution depth low around the pipette minimises pipette capacitance and contributes to reducing noise (Gibb, 1995). External solution was an isotonic high-K$^+$ bath solution of composition (in mM): potassium gluconate 140, KCl 2.5, MgCl$_2$ 1, Hepes 5, EGTA 1.5, pH adjusted to 7.3 with KOH. Capsaicin-evoked activity was observed by applying capsaicin (0.1–0.5 μM) in the pipette solution. The effect of drugs on the single-channel activity in response to capsaicin was studied by exchanging the bath solution. Patch membrane potential was +60 mV relative to the resting membrane potential (assumed to be 0 mV) unless specified otherwise. Junction potentials were cancelled before patch formation, and pipette capacitance was compensated electronically after gigaseal formation. Data were collected with a filtering frequency of 5 kHz (4-pole Bessel filter) and sampling frequency of 20 kHz, or with a filtering frequency of 10 kHz and sampling frequency 50 kHz. For illustrations data were digitally filtered with a Gaussian filter at 1 kHz.

Analysis of single-channel activity

Single-channel recordings were analysed with the pCLAMP 9 suite program Clampfit (Axon Instruments). Data analysis was performed on patches that contained a single channel, and on stretches longer than 40 s. For each capsaicin concentration 10–15,000 events were collected from each of 5–11 separate patches. To determine channel amplitude, all-point amplitude histograms were created using data digitally filtered at 2 kHz. To determine channel open probability and dwell times, traces filtered at 5 kHz were idealised using the half-amplitude threshold crossing method (pCLAMP 9). When using this detection method, the filter has to be set so as to produce an acceptable false event rate, which depends on channel amplitude and standard deviation of the baseline noise, given as root mean square noise. The number of false events per second, λ_f, i.e. the number of times per second that the current departs from the baseline level by more than some

specified amount ϕ, is given approximately by:

$$\lambda_f = f_c \exp\left(-\phi^2/2\sigma_n^2\right) \qquad (1)$$

where λ_f is the number of false events per second, f_c is the filter frequency, ϕ is the 50% threshold amplitude and σ is the standard deviation of the baseline noise (Colquhoun, 1994). Filtering at 5 kHz was adequate for traces for which $\phi/\sigma > 5$, which corresponds to around one false event in 1 min (Colquhoun, 1994; Colquhoun & Sigworth, 1995), and only traces fulfilling this criterion were considered for analysis. As the false event rate depends very steeply on the ratio ϕ/σ, there will be more false events for the open state than predicted, because the open state is noisier than the closed state. Therefore, the idealisation of the trace was monitored visually, and each event inspected before accepting or rejecting it.

To determine the distribution of channel open and closed times, dwell time histograms were created in which the square root of the number of observations N was plotted against the dwell time binned on a logarithmic time scale that contained 10 bins per decade (Sigworth & Sine, 1987; Magistretti *et al.* 2003). The filtering cut-off frequency affects the resolution of the threshold detection method: a Bessel filter with a cut-off frequency of 5 kHz is characterised by a filter risetime (t_r) of 68 μs (Colquhoun & Sigworth, 1995). In order to measure dwell times of events, they must have durations of at least 1.3 t_r, which corresponds to a duration of 88 μs when filtering at 5 kHz (Colquhoun, 1994). For practical analysis, the limit for measurement of durations was set to 100 μs, and events shorter than 100 μs were excluded when fitting the dwell time distribution histograms.

State time constants were obtained from the fit of a sum of exponential functions, each of form $Ae^{-t/\tau}$, where τ is the state time constant and A is a scaling factor, to the dwell time histograms plotted as described above. The variable metric search method in conjunction with the maximum likelihood method was used: the fit converged when the likelihood maximisation does not change by more than a preset value, which was set to 10^{-4}, over at least four iterations (pCLAMP 9, 2003). To determine how many exponential terms best characterise the distribution, an increasing number of terms was used to fit to the data and statistically evaluated; the best model was found when the log likelihood ratio of successive models did not significantly improve. The χ-square statistic was used to evaluate the significance at the specified confidence interval, which was set to 95% (pCLAMP 9, 2003).

The total amount of time spent in each exponentially distributed state is given by

$$\int_0^\infty Ae^{-t/\tau} = A\tau$$

The contribution of each open (or closed) state i to the total open (or closed) time was calculated as $A_i\tau_i/\Sigma A_i\tau_i$, where summation is over all open (or closed) states, and is shown in figures as a percentage.

Reagents

Capsaicin and capsazepine were purchased from Sigma, PMA (phorbol-12-myristate-13-acetate) and staurosporine were purchased from Calbiochem. Stock solutions were prepared in DMSO at a concentration of 5 mM for capsaicin and capsazepine, and 1 mM for PMA and staurosporine, and aliquots were kept at $-20°$C. Cell culture products (culture medium DMEM, fetal bovine serum (FBS), phosphate-buffered saline (PBS) and trypsin-EGTA) were purchased from Gibco.

Statistics

Results are expressed as means $\pm$ standard error of the mean (S.E.M.), with the value of n referring to the number of separate cells on which the experiment was performed. Statistical analysis was performed using Student's unpaired t test.

Results

TRPV1 single-channel activity

Capsaicin (0.25 μM) evokes single-channel activity in transfected cells but not in untransfected control cells, and the capsaicin-induced activity is inhibited by the competitive TRPV1 antagonist capsazepine (Fig. 1*A*). Figure 1*B* shows the relation between membrane voltage and open probability in 0.5 μM capsaicin. Open probability depends on membrane potential, as has been shown in single-channel and whole-cell recordings (Premkumar *et al.* 2002; Voets *et al.* 2004). One feature not apparent from whole-cell recordings, though, is that the channel is not fully opened even at extreme depolarizations ($P_{\mathrm{open,max}} = 0.85$).

Single-channel properties of TRPV1 were determined in detail at three capsaicin concentrations, 0.1, 0.25 and 0.5 μM (see example traces in Fig. 2*A*). To describe single-channel activity the single-channel amplitude, the open probability, P_{open}, and closed and open dwell time distributions were measured. The single-channel amplitude histogram showed two well-separated peaks representing open and closed states, with no sub-conductance levels observed at $+60$ mV (not shown). Single-channel amplitude at $+60$ mV was 5.3 pA, corresponding to a conductance of 88.3 pS, and was unaffected by capsaicin concentration (Fig. 2*B*). Open probability was strongly capsaicin dependent (Fig. 2*C*) but the channel does not open fully even at high capsaicin concentrations.

State time constants were determined by plotting dwell time histograms for open and closed states and by fitting a sum of exponential time constants to the data (see Methods). Figure 3*A* shows representative dwell time histograms for the activity induced by capsaicin at a concentration of 0.1, 0.25 and 0.5 μM in cell-attached patches at +60 mV. At 0.1 μM capsaicin long openings were very infrequent and most open dwell time histograms could be fitted by two time constants, though a third longer component was visible in three recordings. The third component became clearly visible at higher capsaicin concentrations. Open state time constants are shown in Fig. 3*B*. There was no significant effect of capsaicin concentration on any open state time constant. The contribution of the occupancy of each open state to the total open time is shown in Fig. 3*C*. The most prominent effect of increasing capsaicin concentration is that it increases the occupancy of the open state with the longest time constant, O3.

Closed dwell time histograms were well fitted by four time constants at most capsaicin concentrations, with the following exceptions: (i) at the lowest capsaicin concentration, 0.1 μM, a better fit was obtained in 5 cells out of 11 by using two long time constants C4 and C5; (ii) at the highest capsaicin concentration, 0.5 μM, the occupancy of the long closed states became very low and the longest closed state (C4) was clearly distinguished in only 2 out of 5 recordings. The data have been fitted with four time constants in all cases, though we note that Hui *et al.* (2003) distinguished five closed time constants in

similar experiments, as we also noted for some cells at low capsaicin concentrations.

The time constants of the three shorter closed states did not show any significant dependence on capsaicin concentration (all $P > 0.05$). There was also no marked effect of changing capsaicin concentration on the relative occupancy of the three shorter closed states. The time constant of the longest-lived closed state (C4) was by contrast strongly capsaicin dependent, being shortened approximately 5-fold (from 846 ± 85 ms to 179 ± 74 ms) by a 5-fold elevation in capsaicin concentration. The occupancy of the C4 state was also reduced more than 5-fold (from $24 \pm 4\%$ to $3 \pm 0.3\%$) by a 5-fold elevation of capsaicin concentration from 0.1 to 0.5 μM.

Effect of PKC activation on TRPV1 single-channel activity

We activated PKC by applying phorbol myristate acetate (PMA, 0.5 μM) and examined the effect on TRPV1 single-channel activity. PMA is itself a weak activator of TRPV1 (Vellani *et al.* 2001) but at the concentration used here it had no significant effect in directly activating TRPV1 because the effect of PMA was completely abolished by the kinase inhibitor staurosporine or by mutation of specific PKC phosphorylation sites (see below).

Figure 4*A* shows that channel opening in response to 0.1 μM capsaicin was potently enhanced by PKC activation
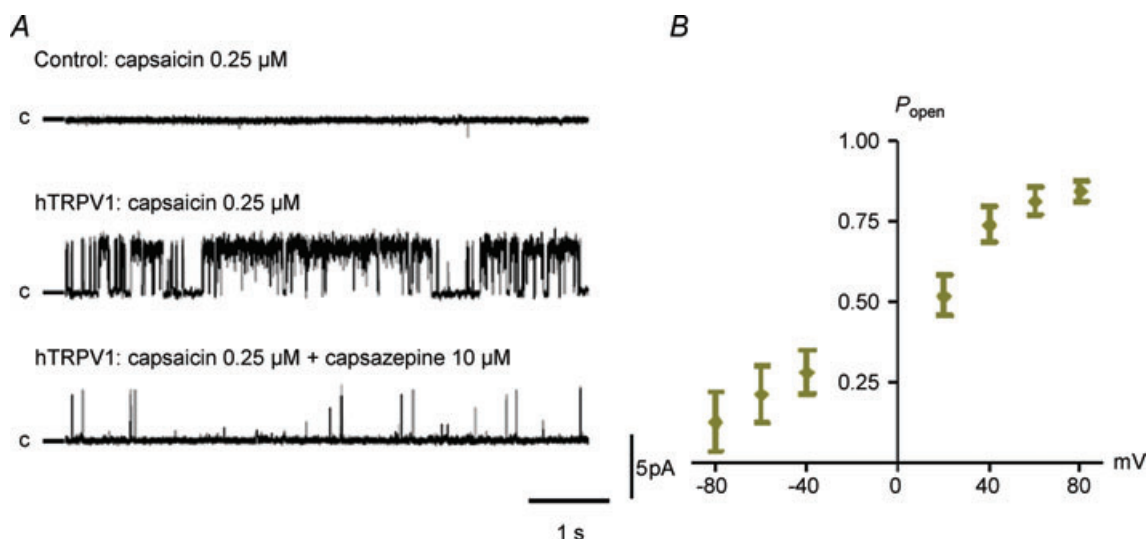
Figure 1. Single-channel activity evoked by capsaicin
A, capsaicin (0.25 μM) applied in the pipette elicits single-channel activity in cell-attached patches from HEK293 cells transfected with hTRPV1 ($P_{open} = 0.446$), but not in non-transfected cells (top). The capsaicin-induced activity is inhibited in the presence of capsazepine (10 μM) in the bath solution (bottom trace, $P_{open} = 0.025$). Single-channel activity was recorded at a membrane potential of +60 mV, openings are upward and c denotes the closed state. *B*, plot of P_{open} vs. voltage shows that the open probability is voltage dependent (capsaicin concentration 0.5 μM; $n = 4$).

in many single-channel recordings. However, in 10 out of 23 patches, some containing multiple channels, PMA had no detectable effect on single-channel activity. The analysis of six traces containing only a single channel, and in which an increase in channel open probability was caused by application of PMA, is summarised in Fig. 4*B* and *C*. The open probability increased within 1 min from 0.082 ± 0.025 to 0.490 ± 0.044 ($n = 6$; ***$P < 0.0001$) with no change in channel conductance (5.17 ± 0.18 pA and 5.20 ± 0.17 pA ($n = 6$) before and after perfusing with PMA, respectively). The effect on the open probability was similar to that of increasing capsaicin concentration to 0.25 μM (see Fig. 2*C*).

Figure 4*B* shows the open and closed dwell time histograms obtained from the example trace in Fig. 4*A*. Open state dwell time analysis of six traces revealed that PMA did not significantly affect the time constant of any

open state (Fig. 5*A* and *B*), but promoted channel opening by increasing the occupancy of the longest-lived open state O3. PMA did not change the time constant or relative occupancies of the shortest three closed states C1 to C3, but reduced the time constant and relative occupancy of the longest lasting C4 state Fig. 5*C* and *D*). Within experimental error these changes in open and closed state occupancy are the same as those of an increase in capsaicin concentration from 0.1 to 0.25 μM (Fig. 3).
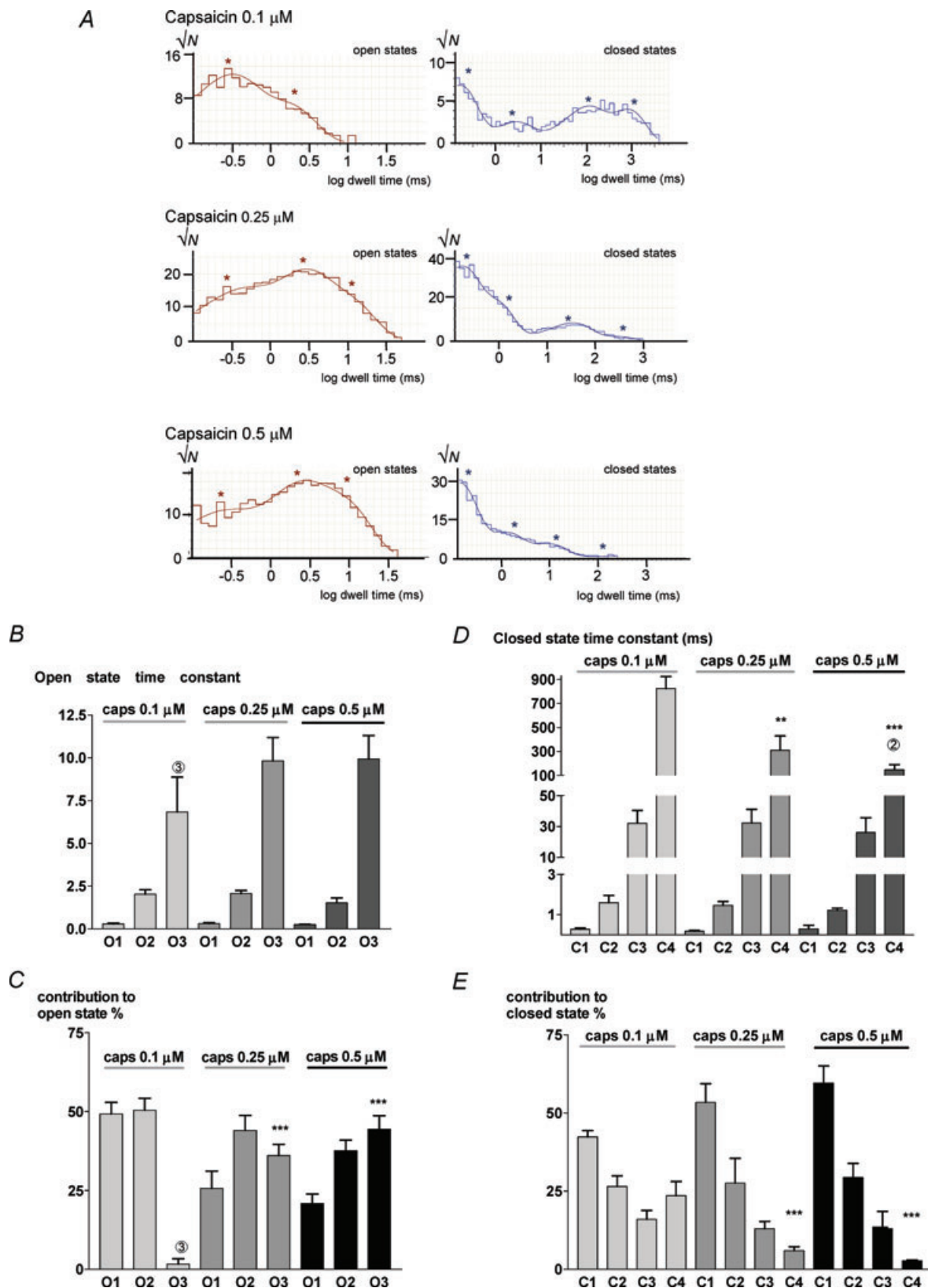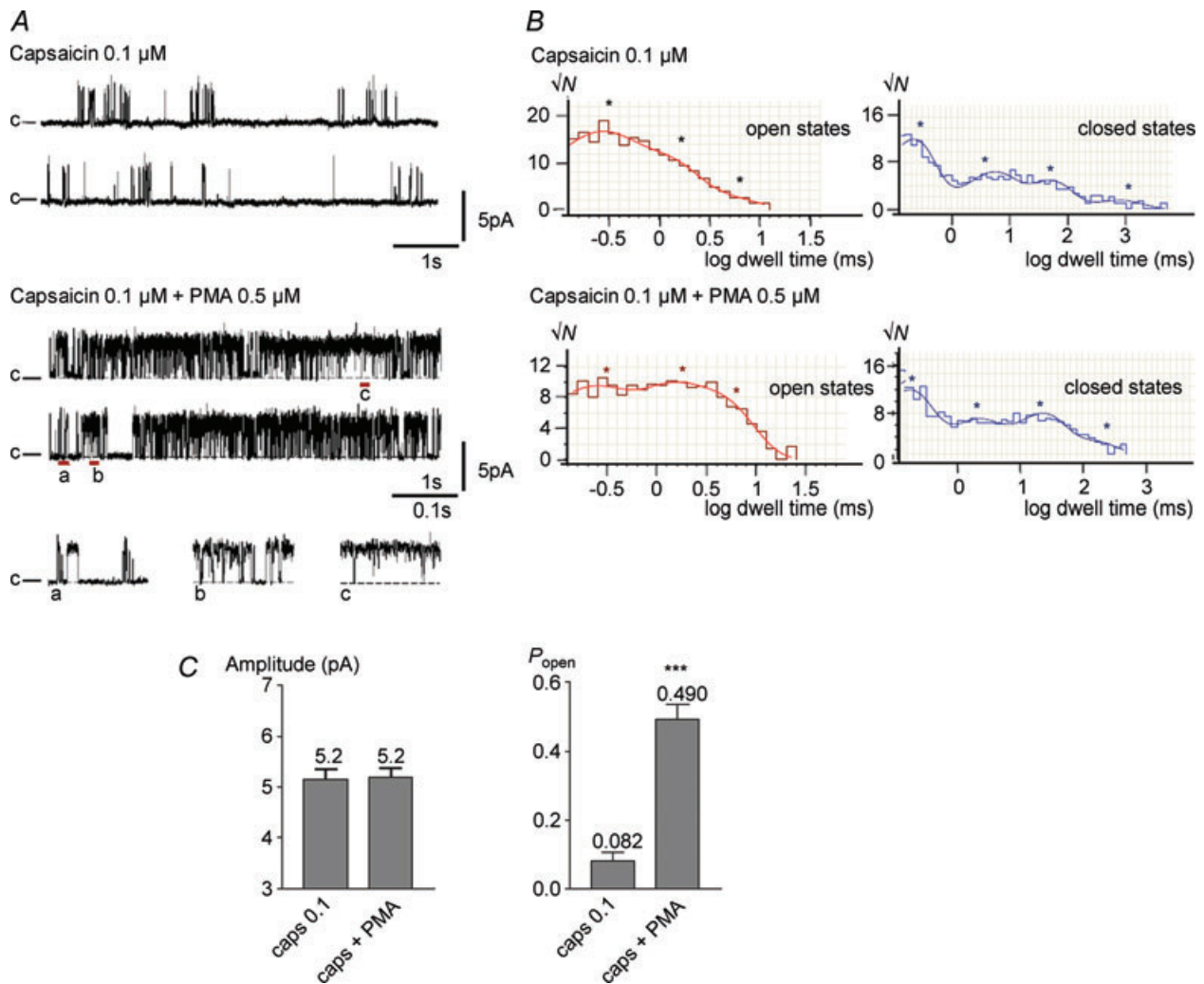
Effect of kinase inhibition on TRPV1 channel activity

The broad-spectrum kinase inhibitor staurosporine inhibits kinases CaMKII, PKC, PKA and PKG with an EC_{50} below 20 nM (Calbiochem, product datasheet). Figure 6*A* shows that staurosporine reduced single-channel activity in the presence of 0.25 μM capsaicin within 1–2 min. Open
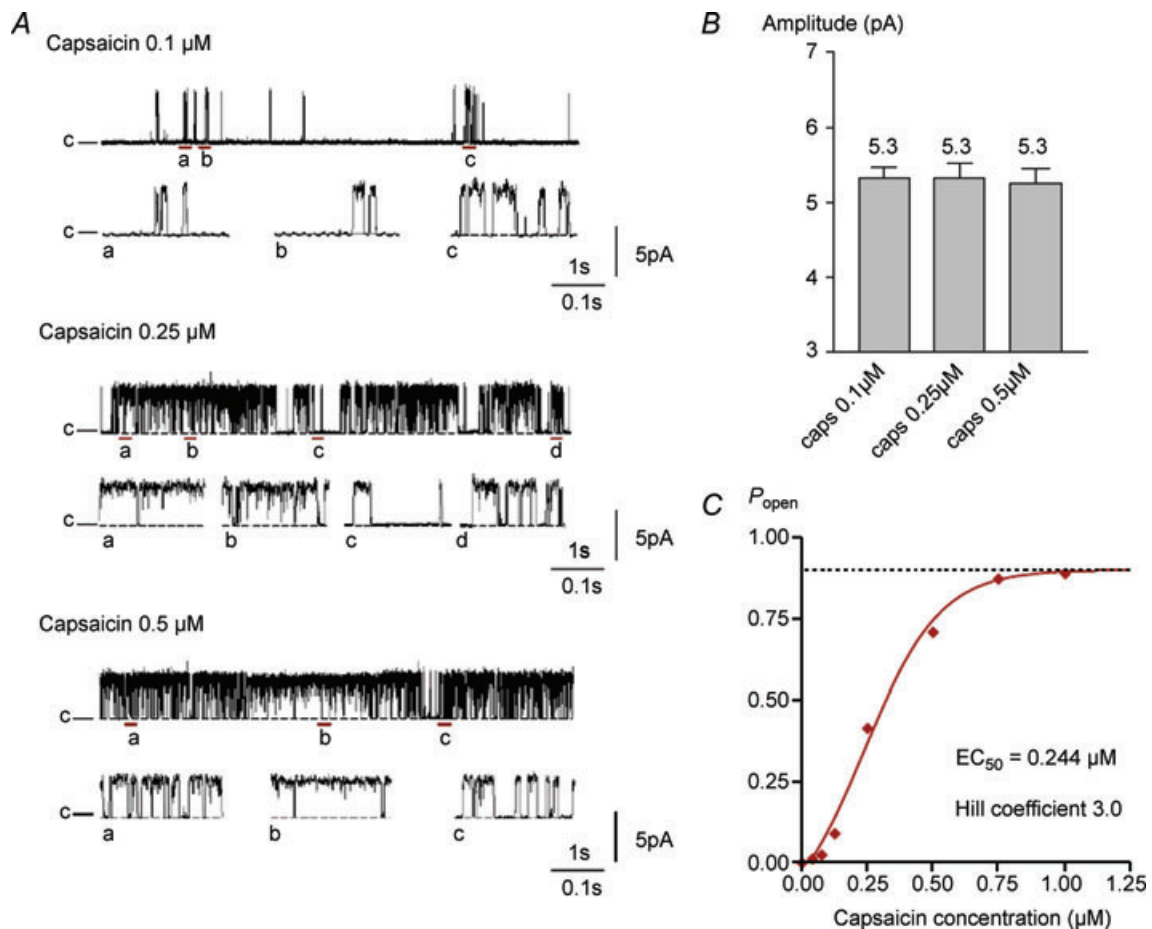
Figure 2. Characteristics of single TRPV1 channels
A, dependence of hTRPV1 single-channel activity on capsaicin concentration (applied in pipette in cell-attached patch configuration). Traces show single-channel activity in response to different capsaicin concentrations (0.1 μM, 0.25 μM and 0.5 μM). c and the dashed line denote the closed level. Fragments of the trace underlined are shown on an expanded time scale below each representative trace for each concentration. *B*, mean single-channel amplitude $\pm$ S.E.M. Numbers of cells (from left) $n = 11$, 5, 5. *C*, dose–response curve obtained in a separate experiment with bath application of capsaicin. The EC_{50} for capsaicin is 0.244 μM, the maximum P_{open} is 0.900 and the Hill coefficient is 3.0.

Figure 3. Capsaicin affects the dwell time distribution of open and closed states

A, dwell time histograms of open (left) and closed states (right). Histograms fitted with sum of exponential components (smooth curves) as detailed in Methods. *Values of time constants used to generate fits. *B*, mean

Figure 4. PMA (0.5 μM) potentiates capsaicin-induced single-channel activity

A, representative traces of single-channel activity induced by 0.1 μM capsaicin and activity recorded from the same cell-attached patch after perfusing PMA. Short stretches are expanded below. *B*, dwell time distribution histograms of the open state (left), and the closed state (right) for activity induced by 0.1 μM capsaicin in the presence and absence of PMA as indicated on the graph. The fit is shown superimposed on the histograms and asterisks indicate the dwell times derived from fitting the dwell time distributions. *C*, bar graphs show mean amplitude ± s.e.m., and average open probability (P_{open}) ± s.e.m. for TRPV1 activity in response to 0.1 μM capsaicin in the presence and absence of PMA. Significance levels: ***$P < 0.001$.

probability was reduced approximately 3-fold with no change in single-channel amplitude (Fig. 6*C*). Analysis of the open and closed state occupancy (see example in Fig. 6*B*) showed that staurosporine reduced occupancy

of the long O3 open state with no change in open state time constants, and increased both the time constant and the occupancy of the long C4 closed state (Fig. 7). These effects are qualitatively similar to those of a reduction in

open state time constants obtained as shown in *A* at three capsaicin (caps) concentrations (mean ± s.e.m.; $n = 11$, 5, 5). The longest time constant at 0.1 μM capsaicin was a minor contributor to the open state time and was only clearly distinguishable in 3 cells (number given above bar in this and other histograms). *C*, percentage contribution of each state to overall channel open time. *D*, closed state time constants as a function of capsaicin concentration. Note piecewise linear scale on ordinate. *E*, contributions of each closed state to the overall closed time. Significance levels: **$P < 0.01$, ***$P < 0.001$ with respect to values in 0.1 μM capsaicin.

capsaicin concentration from 0.25 μM to a value intermediate between 0.1 and 0.25 μM (compare Figs 6 and 7 with Figs 2 and 3).

Figure 6*A* also shows that kinase inhibition with staurosporine completely abolished the effect of PMA in enhancing activation of TRPV1. The open probability following PMA application was indistinguishable from that in the presence of staurosporine alone (Fig. 6*C*). Dwell time analysis also showed no difference in state time constants or occupancy from values observed in the presence of staurosporine alone (data not shown).

Effect of removal of key PKC phosphorylation sites

The phosphorylation sites responsible for PKC-mediated potentiation of TRPV1 were identified as S502 and S801 (residue numbering for hTRPV1, Numazaki *et al.* 2002; Bhave *et al.* 2003). To find out whether constitutively active PKC and phosphorylation of TRPV1 played a role under normal, non-stimulated conditions, the single-channel activity in response to capsaicin of wild type TRPV1 (wt TRPV1) and the TRPV1 S502A/S801A double mutant were compared. Figure 8*A* and *B* (left) shows TRPV1
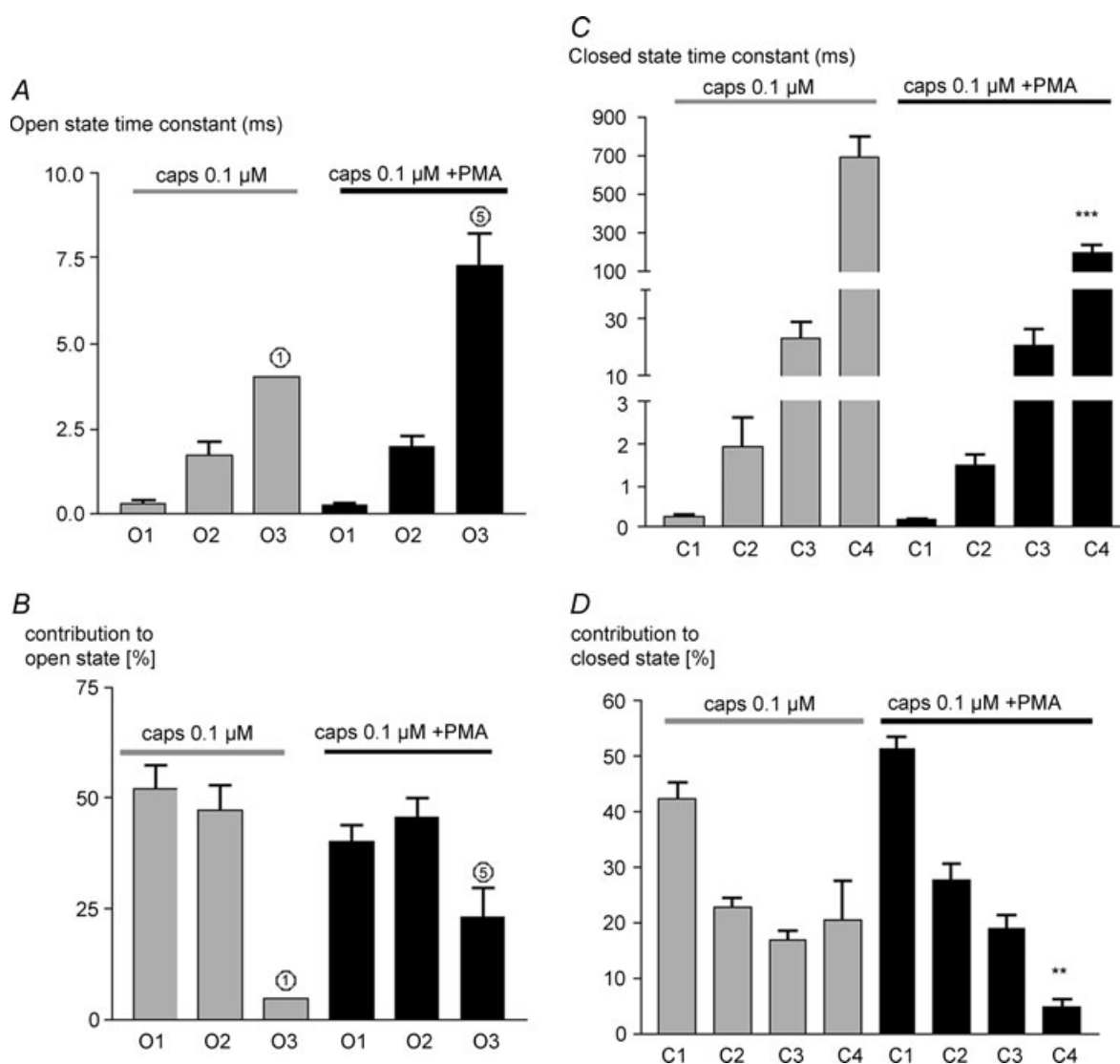

Figure 5. PKC activation with PMA affects state time constants and distribution of open and closed states

A, mean open state time constant ± S.E.M. in response to 0.1 μM capsaicin, and 0.1 μM capsaicin in the presence of PMA. *B*, mean percentage contribution of each open state to total open time. *C* and *D*, similar graphs for closed states. Significance levels: **$P < 0.01$, ***$P < 0.001$ with respect to values in absence of PMA.

S502A/S801A single-channel activity in response to 0.1 μM and 0.25 μM capsaicin. Figure 8C shows that the single-channel conductance and open probability are identical within experimental error to values obtained with wt TRPV1 (see Figs 2 and 3) (t test, $P > 0.05$). Closed and open dwell time analysis at 0.1 μM and 0.25 μM

capsaicin also showed no difference in state time constants or occupancy from values observed with wt TRPV1 (not shown). In particular, there is no sign of the reduced channel activity which was observed in the presence of staurosporine, suggesting that S502 and S801 are not involved in background phosphorylation of TRPV1.
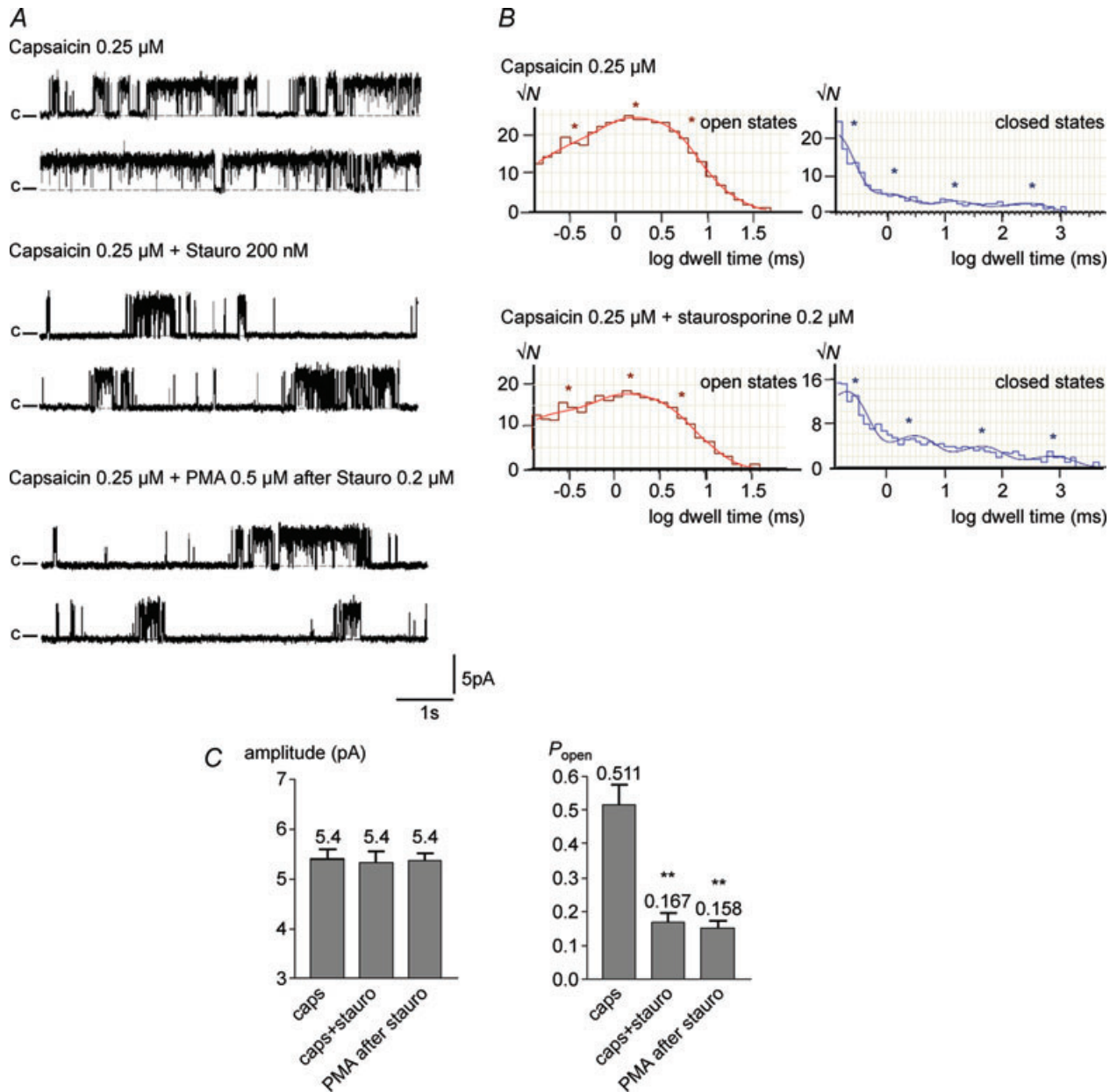
Figure 6. Staurosporine (0.2 μM) reduces capsaicin-induced single-channel activity, and activity does not increase on application of PMA

A, representative traces of single-channel activity induced by 0.25 μM capsaicin; single-channel activity recorded from the same cell-attached patch after perfusing a solution of staurosporine (Stauro, 200 nM); and following application of PMA (0.5 μM). Similar effects observed in 4 out of 5 patches containing single channels. *B*, dwell time distribution histograms of the open state (left) and closed state (right) before and after application of staurosporine. Fit shown superimposed on the graph, and the asterisks denote the dwell times derived from the fit. *C*, mean amplitude ± s.e.m. and open probability (P_{open}) ± s.e.m. in 0.25 μM capsaicin, in 0.25 μM capsaicin plus 200 nM staurosporine, and in PMA (0.5 μM) after treatment with staurosporine. Significance **$P < 0.01$.

We next tested whether PKC activation could potentiate gating of TRPV1 S502A/S801A. Perfusing PMA (0.5 μM) had no effect on S502A/S801A single-channel activity in 5 out of 5 cell-attached patches (Fig. 8*A* right side). Open probability was 0.053 ± 0.018 before and 0.053 ± 0.009 after PMA ($n = 5$), and the burst length 177 ± 52 ms before and 189 ± 60 ms after ($n = 5$). These data confirm at the single-channel level that serines S502 and S801 are crucial for PKC-mediated modulation of TRPV1.

The effect of general kinase inhibition using staurosporine was also assessed on TRPV1 S502A/S801A. Single-channel activity was inhibited by staurosporine to a similar extent to the inhibition observed in the case of wt TRPV1 (Fig. 8*B*, right). Staurosporine reduced the open probability from 0.571 ± 0.044 to 0.145 ± 0.078 ($n = 2$; *$P = 0.0413$), and the burst length from 2027 ± 441 ms to 289 ± 59 ms ($n = 2$).

Discussion

The aim of this study was to elucidate the mechanism of modulation of TRPV1 gating by phosphorylation. We first characterised state time constants and occupancy of the closed and open states of TRPV1 in the presence of capsaicin. Our results are in agreement with the more complete study carried out by Hui *et al.* (2003), who identified five closed states in long recordings at low capsaicin concentrations. In our recordings we could clearly identify only four closed states, with evidence in
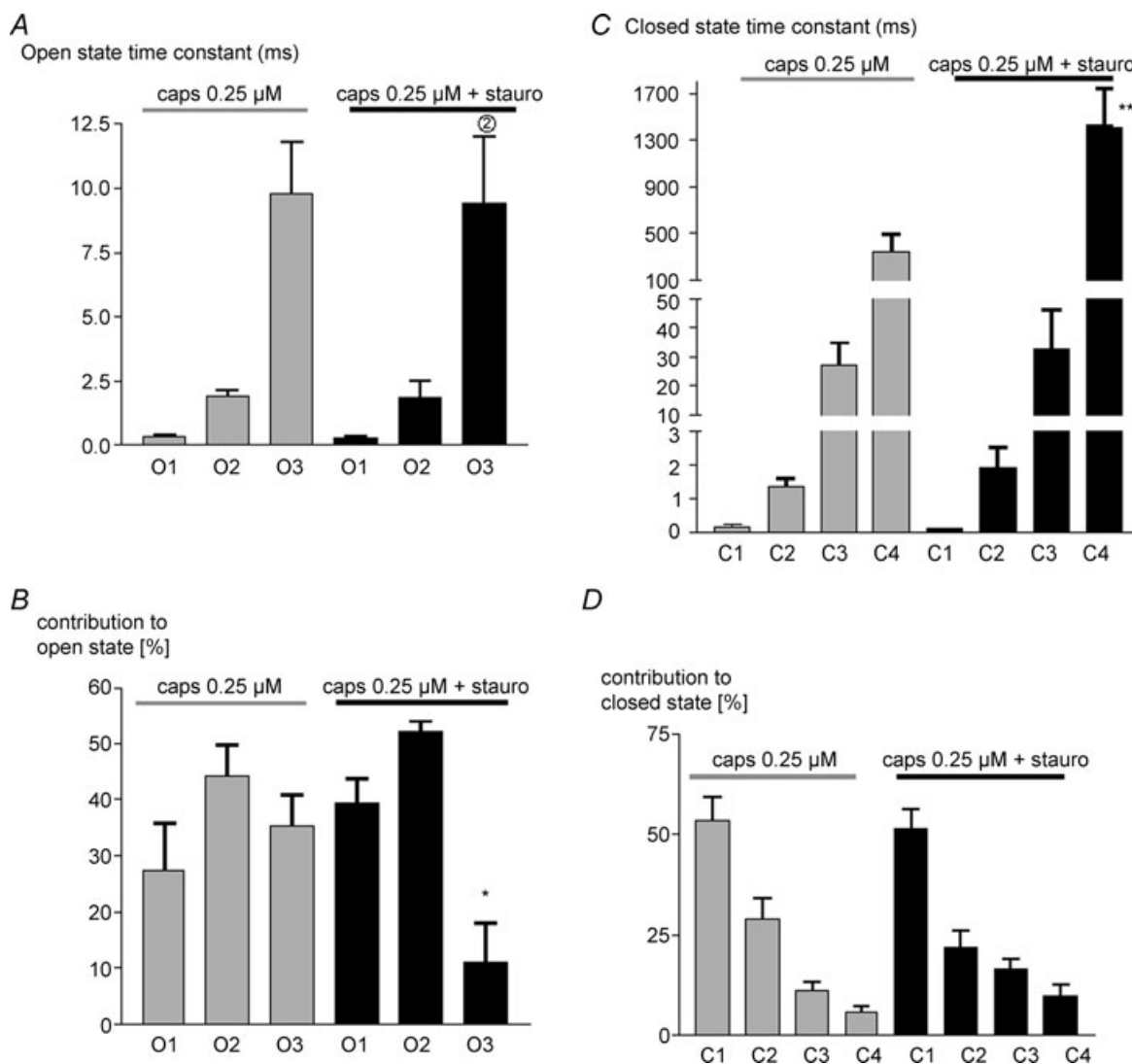
Figure 7. Staurosporine affects dwell time distribution of open and closed states
*A*, mean open state time constants $\pm$ S.E.M. with 0.25 μM capsaicin alone, and with 0.25 μM capsaicin in presence of 0.2 μM staurosporine. *B*, mean percentage contribution of each open state to the total open time. *C* and *D*, similar graphs for closed dwell times. Significance levels: *$P < 0.05$, **$P < 0.01$ with respect to values in absence of staurosporine.

some experiments to suggest a fifth long closed state, so we used four closed states to fit all experiments. Increasing capsaicin concentration shortened the time constant and reduced the occupancy of the long closed state, C4, with a 5-fold increase in capsaicin causing an approximately 5-fold reduction in both time constant and relative state occupancy. Increasing the capsaicin concentration had no marked effect on either the time constants or the relative occupancy of the other three shorter-lived closed states. Three open states were clearly distinguished. Capsaicin promoted occupancy of the longest open state relative to the others, but in an apparent paradox, increasing capsaicin concentration had no significant effect on time constants of any of the open states.

In a multi-state model each state time constant is the inverse of the sum of the rates of exit from the state. For example for state S2 in Fig. 9A:

$$\text{Time constant} = (\beta_1 + \alpha_2)^{-1}$$

If capsaicin binds to S2 to form state S3 then $\alpha_2 = k[\text{caps}]$, where k is a constant, and both state occupancy and time constant will therefore decrease as capsaicin concentration ([caps]) increases. Thus, a first-order binding of one capsaicin molecule to the long closed state C4 provides an explanation for the parallel decrease in both time constant and occupancy of this state when the capsaicin concentration is increased. The simplest explanation for activation of TRPV1, which is a tetrameric channel composed of identical subunits, would be that the transition between each closed state is due to the binding of one further capsaicin, and that each state would then exhibit a similar dependence to C4 of both time constant and occupancy on capsaicin concentration. The experimental data clearly fail to support this idea.
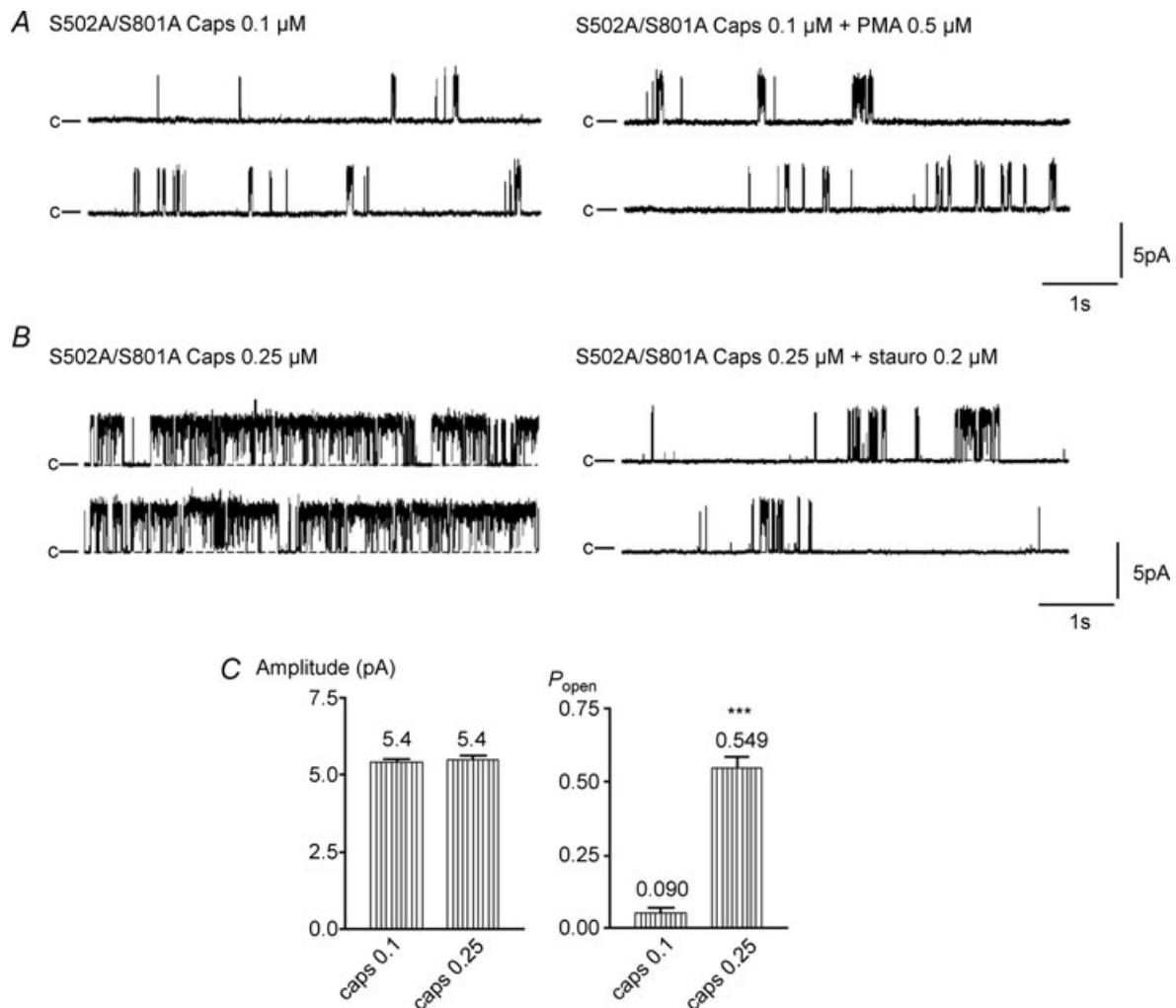
Figure 8 Effect of deletion of critical PKC phosphorylation sites
Modulation of TRPV1 S502A/S801A activity by PMA (*A*, 0.1 μM) and staurosporine (*B*, 0.2 μM). *C*, mean amplitude $\pm$ S.E.M. and average open probability (P_{open}) $\pm$ S.E.M. for S502A/S801A activity in response to 0.1 and 0.25 μM capsaicin. Significance ***$P < 0.001$.

A simple model to explain agonist-dependent changes in protein conformation is the Monod–Wyman–Changeux model in which the agonist can bind to every state in each of two channel configurations, either closed or open (MWC model, Fig. 9*B*). Agonist binding promotes opening by shifting occupancy to states to the right of the diagram, where transitions from closed to open states are more likely. As noted above, the model predicts that time constants and occupancies of all states apart from C1 and O3 will depend on agonist concentration, and is therefore not consistent with the single-channel data for TRPV1 because time constants for all open states, and all closed states apart from C4, are agonist independent. A simple modification is to remove agonist binding to all states apart from C4 (Fig. 9*C*). This model accounts for the behaviour of the closed states, for which both occupancies and time constants are all agonist independent apart from C4. It also accounts for the lack of dependence on agonist concentration of the open state time constants, but it does not account for the increase in long open state (O3) occupancy as capsaicin concentration is increased, and is also not consistent with binding of four capsaicin molecules to the identical subunits of the tetrameric TRPV1. A further modification which would explain the prominent dependence on capsaicin concentration of the occupancy of the long O3 state is to postulate a

'hidden' capsaicin-binding state O* between O2 and O3 (see Fig. 9*D*), which is not detected either because of low occupancy or because the dwell time constant is too short for the recording bandwidth. This model accounts for the single-channel data in qualitative terms but must be an over-simplification because it includes only two instead of four capsaicin binding steps. However, the model has the important feature, which seems to us inescapable, that channel openings can occur from partially liganded states. A similar conclusion was reached by Hui *et al.* (2003).

TRPV1 modulation by phosphorylation

We next examined the effect of activation of PKC on TRPV1 single-channel gating. Although the non-physiological agonist capsaicin was used throughout, we expect the results to be applicable to activation of PKC by other agonists such as protons and anadamide, and by physical stimuli such as heat and membrane stretch, because the activation of TRPV1 and other members of the TRPV family is potentiated by phosphorylation in a manner which appears to be independent of the activator (Vellani *et al.* 2001; Fan *et al.* 2009).

TRPV1 single-channel activity in response to capsaicin was found to be potently enhanced by PKC activation (Fig. 4*A*). There was no change in single-channel conductance, and all the increase in current flowing through an individual channel can be therefore attributed to an increase in channel opening probability (Fig. 4*C*). The effect on the open probability was similar to that of an increase in capsaicin concentration by a factor of 2.5 (compare Fig. 4*C* with Fig. 2*C*). This finding is in agreement with the observation that activation of PKC causes an approximately 2-fold shift in the whole-cell dose–response curve for TRPV1 activation by capsaicin (Vellani *et al.* 2001).

The majority of channels responded to PKC activation with an increase in channel opening but around a third were insensitive. Whole-cell currents do not show a similar variability (Vellani *et al.* 2001). We have recently shown that potentiation of TRPV1 by PKC depends on the scaffolding protein AKAP79 (Zhang *et al.* 2008), and a possible explanation for the diversity in response to PKC at the single-channel level may be that some channels have PKC pre-assembled in a signalling complex by AKAP79, and are therefore phosphorylated when PKC is activated, while other channels do not have AKAP79 bound to them and therefore are inaccessible to phosphorylation by PKC.

The results described here show clearly that the activity of single channels is potentiated by phosphorylation, but they do not exclude other mechanisms for potentiation of TRPV1, such as enhanced trafficking of channels to the membrane. Activation of PKC or the non-receptor
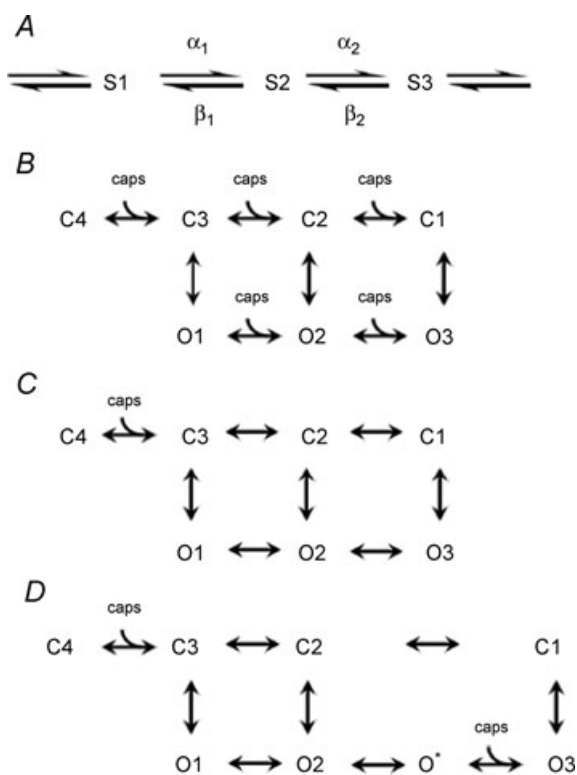
Figure 9. Possible state diagrams for TRPV1
Explanation in text.

tyrosine kinase Src are known to rapidly increase expression of functional channels in the membrane by promoting movement of channels from a subcellular compartment (Morenilla-Palao *et al.* 2004; Zhang *et al.* 2005). This mechanism is an important contributor to heat hyperalgesia but was not observed with the experimental methods used in the present study, in which single channels are trapped under a recording pipette and the addition of further channels into the small patched area of membrane would be a rare event.

Figure 5 shows that PKC activation has two main effects: (i) to shorten the time constant and decrease the occupancy of the long C4 closed state, and (ii) to increase the occupancy of the long O3 open state relative to the other open states, with no significant change in time constant. These changes are identical within experimental error to those seen with a 2.5-fold increase in capsaicin concentration (Fig. 3*B–D*). Thus, the simplest explanation would be that phosphorylation enhances the affinity of capsaicin binding, perhaps by inducing a conformational change in the capsaicin binding site. One key PKC phosphorylation site, S502, is located on the intracellular loop between helices 2 and 3, close to the capsaicin binding site which is centred on Y511/S512 (Jordt & Julius, 2002). The additional negative charge conferred by phosphorylation could therefore directly promote a conformational change which facilitates capsaicin binding to TRPV1.

This explanation is not obviously applicable, however, to the second site known to be relevant for PKC-mediated phosphorylation, S801, which in terms of amino acid sequence is located in the C-terminal tail of the molecule, some distance away from the capsaicin binding site. A second problem with the idea that phosphorylation simply increases the affinity for capsaicin is that phosphorylation acts in a similar way to enhance the activation of TRPV1 by a wide range of agonists which bind to sites located in different parts of the molecule, and to heat, whose site of action is unknown (Vellani *et al.* 2001). Protons are known to act at an extracellular location (Jordt *et al.* 2000; Ryu *et al.* 2003) while the site of capsaicin binding is intracellular (Jung *et al.* 1999; Jordt & Julius, 2002). Because of the substantial separation between the known locations of capsaicin and proton binding sites, it seems unlikely that a simple change of conformation at the capsaicin binding site could explain the similar effects of phosphorylation on activation by both capsaicin and protons. We conclude that a change in affinity of the capsaicin binding site is not a likely explanation for the increase in channel open probability following phosphorylation, and the action is instead on downstream steps leading to channel opening.

The serine–threonine kinase inhibitor staurosporine reduced single-channel activity by increasing the duration of the long C4 closed state and reducing occupancy of the long O3 open state (Figs 6 and 7). These effects are the opposite of those observed following phosphorylation, and resemble the effects of a reduction in capsaicin concentration.

Role of key PKC phosphorylation sites on TRPV1

The double mutant TRPV1 S502A/S801A, in which the key PKC phosphorylation sites have been replaced by alanines, was used to assess the importance of PKC phosphorylation at these two sites under non-stimulated conditions and in response to PMA. There was no difference in single-channel activity in response to capsaicin between wt TRPV1 and TRPV1 S502A/S801A when comparing amplitude, open probability and dwell time distribution. Treatment with staurosporine reduced the activity and changed the dwell time distribution for both wt TRPV1 and TRPV1 S502A/S801A to a similar degree, demonstrating that basal phosphorylation at sites other than these two causes channel potentiation in the resting cell. However, the activity of the double mutant was not potentiated by PMA, confirming other studies showing that these two sites are key for PKC action (Numazaki *et al.* 2002; Bhave *et al.* 2003). When taken together, these data give evidence that the potentiating effect of PKC on TRPV1 single-channel activity is caused by phosphorylation of serines S502 and S801, but that phosphorylation by other kinases and at other locations also modulate TRPV1, and that activity of these kinases in the unstimulated cell causes a degree of basal sensitization of TRPV1.

References

Bhave G, Hu HJ, Glauner KS, Zhu W, Wang H, Brasier DJ, Oxford GS & Gereau RW (2003). Protein kinase C phosphorylation sensitizes but does not activate the capsaicin receptor transient receptor potential vanilloid 1 (TRPV1). *Proc Natl Acad Sci U S A* **100**, 12480–12485.

Caterina MJ, Leffler A, Malmberg AB, Martin WJ, Trafton J, Petersen-Zeitz KR, Koltzenburg M, Basbaum AI & Julius D (2000). Impaired nociception and pain sensation in mice lacking the capsaicin receptor. *Science* **288**, 306–313.

Caterina MJ, Schumacher MA, Tominaga M, Rosen TA, Levine JD & Julius D (1997). The capsaicin receptor: a heat-activated ion channel in the pain pathway. *Nature* **389**, 816–824.

Colquhoun D (1994). Practical analysis of single channel records. In *Microelectrode Techniques, The Plymouth Workshop Handbook*, ed. Odgen D, pp. 101–139. The Company of Biologists Limited, Cambridge.

Colquhoun D & Sigworth, D (1995). Fitting and statistical analysis of single channel records. In *Single Channel Recording*, eds Sakmann B & Neher E, pp. 483–587. Plenum Press, New York.

Davis JB, Gray J, Gunthorpe MJ, Hatcher JP, Davey PT, Overend P *et al.* (2000). Vanilloid receptor-1 is essential for inflammatory thermal hyperalgesia. *Nature* **405**, 183–187.

Fan HC, Zhang X & McNaughton PA (2009). Activation of the TRPV4 ion channel is enhanced by phosphorylation. *J Biol Chem* **284**, 27884–27891.

Gibb AJ (1995). Patch-clamp recording. In *Ion Channels: A Practical Approach*, ed. Ashley RH, pp. 1–42. Oxford University Press, Oxford.

Huang J, Zhang X & McNaughton PA (2006). Modulation of temperature-sensitive TRP channels. *Semin Cell Dev Biol* **17**, 638–645.

Hui K, Liu B & Qin F (2003). Capsaicin activation of the pain receptor, VR1: multiple open states from both partial and full binding. *Biophys J* **84**, 2957–2968.

Jordt SE & Julius D (2002). Molecular basis for species-specific sensitivity to "hot" chili peppers. *Cell* **108**, 421–430.

Jordt SE, Tominaga M & Julius D (2000). Acid potentiation of the capsaicin receptor determined by a key extracellular site. *Proc Natl Acad Sci U S A* **97**, 8134–8139.

Jung J, Sun WH, Kwak J, Lee S-Y, Kang C-J, Won BK, Kim D & Oh U (1999). Capsaicin binds to the intracellular domain of the capsaicin-activated ion channel. *J Neurosci* **19**, 529–538.

Liu B, Hui K & Qin F (2003). Thermodynamics of heat activation of single capsaicin ion channels VR1. *Biophys J* **85**, 2988–3006.

Magistretti J, Ragsdale DS & Alonso A (2003). Kinetic diversity of single-channel burst openings underlying persistent Na^+ current in entorhinal cortex neurons. *Biophys J* **85**, 3019–3034.

Morenilla-Palao C, Planells-Cases R, Garcia-Sanz N & Ferrer-Montiel A (2004). Regulated exocytosis contributes to protein kinase C potentiation of vanilloid receptor activity. *J Biol Chem* **279**, 25665–25672.

Numazaki M, Tominaga T, Toyooka H & Tominaga M (2002). Direct phosphorylation of capsaicin receptor VR1 by protein kinase $C\varepsilon$ and identification of two target serine residues. *J Biol Chem* **277**, 13375–13378.

pClamp 9 (2003). Clampfit curve fitting. In *pCLAMP 9 User's Guide*, pp. 249–313. Axon Instruments.

Premkumar LS, Agarwal S & Steffen D (2002). Single-channel properties of native and cloned rat vanilloid receptors. *J Physiol* **545**, 107–117.

Premkumar LS & Ahern GP (2000). Induction of vanilloid receptor channel activity by protein kinase C. *Nature* **408**, 985–990.

Ryu S, Liu B & Qin F (2003). Low pH potentiates both capsaicin binding and channel gating of VR1 receptors. *J Gen Physiol* **122**, 45–61.

Sigworth FJ & Sine SM (1987). Data transformations for improved display and fitting of single-channel dwell time histograms. *Biophys J* **52**, 1047–1054.

Tominaga M, Caterina MJ, Malmberg AB, Rosen TA, Gilbert H, Skinner K, Raumann BE, Basbaum AI & Julius D (1998). The cloned capsaicin receptor integrates multiple pain-producing stimuli. *Neuron* **21**, 531–543.

Vellani V, Mapplebeck S, Moriondo A, Davis JB & McNaughton PA (2001). Protein kinase C activation potentiates gating of the vanilloid receptor VR1 by capsaicin, protons, heat and anandamide. *J Physiol* **534**, 813–825.

Voets T, Droogmans G, Wissenbach U, Janssens A, Flockerzi V & Nilius B (2004). The principle of temperature-dependent gating in cold- and heat-sensitive TRP channels. *Nature* **430**, 748–754.

Zhang X, Huang J & McNaughton PA (2005). NGF rapidly increases membrane expression of TRPV1 heat-gated ion channels. *EMBO J* **24**, 4211–4223.

Zhang X, Li L & McNaughton PA (2008). Proinflammatory mediators modulate the heat-activated ion channel TRPV1 via the scaffolding protein AKAP79/150. *Neuron* **59**, 450–461.

Zygmunt PM, Petersson J, Andersson DA, Chuang HH, Sorgard M, Di Marzo V, Julius D & Hogestatt ED (1999). Vanilloid receptors on sensory nerves mediate the vasodilator action of anandamide. *Nature* **400**, 452–457.

Author contributions

M.S. planned and carried out experiments, analysed and interpreted data, and drafted the manuscript. P.A.M. designed the project, advised on experiments, analysed and interpreted data and wrote the final version, which was approved by both authors.

Acknowledgements